Magmatic activity beneath the quiescent Three Sisters volcanic center, central Oregon Cascade Range, USA

Charles W. Wicks Jr[1], Daniel Dzurisin[2], Steven Ingebritsen[1], Wayne Thatcher[1], Zhong Lu[3], and Justin Iverson[4]

Abstract. Images from satellite interferometric synthetic aperture radar (InSAR) reveal uplift of a broad ~10 km by 20 km area in the Three Sisters volcanic center of the central Oregon Cascade Range, ~130 km south of Mt. St. Helens. The last eruption in the volcanic center occurred ~1500 years ago. Multiple satellite images from 1992 through 2000 indicate that most if not all of ~100 mm of observed uplift occurred between September 1998 and October 2000. Geochemical (water chemistry) anomalies, first noted during 1990, coincide with the area of uplift and suggest the existence of a crustal magma reservoir prior to the uplift. We interpret the uplift as inflation caused by an ongoing episode of magma intrusion at a depth of ~6.5 km.

Introduction

In central Oregon the Cascade Range is a volcanic highland or platform formed by eruptions from hundreds of volcanic vents rather than just a few isolated volcanic centers [*Bacon*, 1985; *Guffanti and Weaver*, 1988; *Scott et al.*, 2001; *Sherrod and Smith*, 1990]. The most recent eruptions in the Three Sisters volcanic center produced flows of basaltic lava ~1,500 years ago, and flows of rhyolitic lava ~2,000 years ago [*Taylor et al.*, 1987]. Surficial Quaternary volcanics in the Three Sisters area (Fig. 1) are mostly bare rock to lightly vegetated and the European Space Agency Earth Resource Satellites (ERS-1 and ERS-2) archive of data over the area is fairly deep. The Three Sisters volcanic center is, therefore, an attractive target to search for possible volcano related deformation using InSAR techniques. Image pairs for the period 1992-2000 used in this study were selected based on orbital separation and optimal (most snow-free) time of year.

InSAR Observations and Modeling

The interferograms in Fig. 2 and range change profiles derived from them (Fig. 3) show that any deformation prior to 1998 was very small. The pattern of motion immediately west of South Sister is evident in Figs. 2d, e and f, which span 1995-2000, and is small or absent in Figs. 2a, b and c, which cover 1992-1998. We formed interferograms by calculating the phase difference between two satellite images, then using a digital elevation model (DEM) to remove the topographic contribution from the interferogram [*Massonnet and Rabaute*, 1993]. The resulting interferograms are maps of the change in line-of-sight distance (or range) between ground points and an orbiting satellite, during the time interval spanned by two radar data acquisitions. We used precise Delft orbits [*Scharroo and Visser*, 1998] to calculate all the interferograms, and applied an orbital error correction only to the interferogram in Fig. 2d where fringes with the appearance of orbital errors have been removed by subtracting a best-fit plane. In Fig. 2, no measurable deformation is found before 1996 and up to ~30 mm of range change is apparent from 1996 to 1998. Deformation began or accelerated after the autumn of 1998 at a rate of ~30-50 mm/yr (Figs. 2c, 2d, and 3) and the sense of motion is towards the satellite. Since the observations are most sensitive to vertical motions, the signal most likely indicates uplift. The data shown are all from descending orbits and the satellite unit look vector is (0.34, -0.08, 0.94) in the direction (east, north, up). The uplift continued at a rate of ~30-50 mm/yr from the autumn of 1999 to the time of the last measurement in the autumn of 2000 (Figs. 2e, 2f, and 3).

We have modeled the three interferograms shown in Figs. 2d, 2e, and 2f with an inflating point source [*Mogi*, 1958] that includes a correction to account for topographic variation [*Williams and Wadge*, 1998] and a tropospheric correction [*Avallone and Briole*, 2000]. The interferogram in Fig. 2f has the largest apparent signal to noise ratio, so we show the results of modeling it in Fig. 4. Although the unwrapped interferogram was modeled, wrapped versions are shown here to better reveal small-scale features of the deformation fields.

First we modeled the data (Fig. 2f) with a seven-parameter model consisting of a point source [*Mogi*, 1958] (x and y location, depth and volume change, planar phase gradients in the x and y directions, and a static shift between the model and the data). In addition we have employed a simple method that has been shown [*Williams and Wadge*, 1998] to be an improvement over the elastic half-space assumption, by correcting for topographic variation through a variable source depth that accounts for the difference in elevation of the different data points. In this first modeling effort, the best-fit planar phase gradient parameters that account for orbital errors were unrealistically large (~60 mm across-track for the whole 100 km by 100 km scene). No orbital fringes were seen in the whole scene interferogram, so the model (Fig. 4b) is not satisfactory.

Inspection of the data in Fig. 4a (also shown in Fig. 1 and Fig. 2f) revealed that fringes follow topography outside of the deforming area, so an additional parameter to allow a simple troposphere correction was added to the inversion. We assumed a linear change in range with change in elevation for the troposphere correction. This is equivalent to (for example) a change in the thickness of the troposphere [*Tarayre and Massonnet*, 1996] and it is similar to the troposphere correction used in other studies [for example, *Avallone and Briole*, 2000]. The resulting best-fit model enabled a better fit to the data than found in Fig. 4b and yielded realistic values for orbital fringe gradients across the whole 100 km by 100 km scene (~1/2 a fringe in N-S and E-W directions). A source at a depth of 6.5 – 0.4 km with a volume increase of 0.023 – 0.003 km^3 provides an adequate fit to the data (Fig. 4f). About 10 to 20 times this volume was erupted from Mount St. Helens in May 1980. Modeling results of 30 m pixel versions of the interferograms in Fig. 2d and 2e yield depths ~1 km shallower. The depth difference may result from unaccounted for atmospheric artifacts.

Geochemical Anomalies

A U. S. Geological Survey (USGS) geothermal reconnaissance in the central Oregon Cascades [*Ingebritsen et al.*, 1988; *Ingebritsen et al.*, 1994] included water samples of ~800 streams, springs, and wells from ~44ß N to 45.25ß N. Within the Quaternary volcanic arc of central Oregon, anomalously high chloride fluxes (~10 g/s Cl) were found only in Separation Creek -- all other large chloride fluxes are related to thermal springs associated with older rocks of the Western Cascades at lower elevations. The chloride-ion concentrations and fluxes of the waters were of particular interest because thermal waters of the Cascades are rich in chloride, which generally does not get taken up by water-rock reactions, whereas the streams are generally very dilute (<0.7 mg/L Cl). Because chloride does not enter into water-rock reactions, it tends to stay in solution to near halite concentration. Additional field studies [*Iverson*, 1999] confirmed that the source of the anomaly is coincident with the area of peak uplift (Fig. 1). A positive correlation between chloride concentration and spring temperature, as well as larger SO_4/Cl ratios in springs at higher elevations (Fig. 1) were also found [*Iverson*, 1999]. The chloride-temperature correlation suggests a hydrothermal source for the chloride, and the positive correlation between the SO_4/Cl ratio and elevation suggests phase separation at depth [*White et al.*, 1971], indicative of a high-temperature hydrothermal system driven by magmatic intrusions.

Preliminary results of a helicopter survey in April 2001 suggest slightly elevated concentrations of CO_2 in air ~60 m above the upper reach of Separation Creek, in the vicinity of the high-Cl springs (Doukas, Cascades Volcano Observatory, USGS, personal communication). This suggests the presence of a degassing magma body in the upper crust, consistent with both the uplift observations and models, and the water chemistry anomalies outlined above. Additional CO_2 is likely captured by the cold groundwater system; dissolved magmatic carbon measured in cold springs east of the Three Sisters has been shown to indicate magmatic CO_2 fluxes comparable to those in recently active volcanic centers [*James et al.*, 1999].

Discussion

We interpret the inflation to be either the result of intrusion of magma at depth, or pressurization of a sealed geothermal system similar to, but necessarily much smaller than the one interpreted at Yellowstone caldera [*Wicks et al.*, 1998]. However, such geothermal systems tend be associated with persistent or sporadic seismicity and conspicuous surface manifestations such as hot springs or thermal pools, both of which are missing at Three Sisters. Although the Three Sisters volcanic center is historically aseismic, the central Oregon Cascades are only sparsely instrumented with seismometers, so small earthquakes could escape detection. Aseismic inflation, however, has also been observed with InSAR at two arc volcanoes in the Aleutians: Westdahl [*Lu et al.*, 2000] with documented eruptions in 1964, 1978-79, and 1991-92; and Peulik [*Lu et al.*, 2001], which has not erupted in ~150 years. Westdahl is a large shield volcano that began inflating rapidly at a depth of ~9 km after an eruption in 1990-91. Peulik is a stratovolcano more like South Sister (the youngest of the stratovolcanoes in the Three Sisters volcanic center). The interferograms of Peulik revealed ~0.05 km^3 of magma accumulated at a depth of ~7 km during an inflation episode in 1996-98, a period that included a strong earthquake swarm ~30 km to the northwest, but no unusual seismicity beneath the volcano.

The inflation sources at Peulik and Three Sisters are at similar depths, and the aseismic nature of the episodes suggests that magma accumulated near the brittle-ductile transition beneath both volcanoes. Such episodes of magma injection might be common at volcanic centers and, in some cases, eventually lead to eruptions. Many intrusions undoubtedly cool, however, and crystallize entirely without reaching the surface, thereby adding to subvolcanic intrusive complexes. Whether volcanic eruptions occur as a result of many small incremental intrusions or fewer larger intrusions is not known.

The inferred intrusion of magma may be basaltic to rhyolitic in composition, as represented by erupted material in the area. Although the silicic system identified around South Sister is relatively small [*Bacon*, 1985], the production and maintenance of partial melts in the crust over an extended time period to feed the surface distribution of silicic vents requires a persistent heat source — presumably repeated intrusions of basaltic magma. There are also hundreds of small basaltic late Quaternary volcanic vents (nearly contemporaneous with the silicic vents) in the Three Sisters area [*Bacon*, 1985; *Guffanti and Weaver*, 1988], so influx of basaltic magma to the upper crust must occur, at least episodically. The mean magmatic intrusion rates estimated from heat-flow are ~9 to 50 km^3/Ma per kilometer of arc length [*Blackwell et al.*, 1990; *Ingebritsen et al.*, 1989]. If we assume an effective arc length of ~20 km for the Three Sisters center, 0.02 km^3 should be injected there every 20-100 years.

Whether the inflation at Three Sisters will soon lead to an eruption is not known. Hazards that future eruptions will pose have been assessed from the geologic record of past eruptive activity [*Scott et al.*, 2001]. The style of eruption could be explosive to effusive, depending mainly on the composition of erupting magma. If the current inflation episode is similar to that observed at Peulik, then we would expect the inflation to cease in the next year or two. If inflation continues and shallow earthquakes start to occur, especially long-period earthquakes that indicate pressurization or migration of fluids, then an eruption may soon follow. If inflation ceases, we must continue monitoring the area in anticipation of the next intrusive event. (**Note Added in Proof:** Additional interferograms using autumn 2001 scenes show that uplift has continued into autumn 2001 and continuous GPS data, from a station near the center of deformation, indicate uplift has continued into January 2002.) The more persistent geochemical anomaly suggests that the inflation episode is likely the latest in a series of hitherto undetected magma intrusions. Continued long term monitoring of the Three Sisters volcanic center might yield valuable insight into the eruption cycles of this center and, by generalization, other quiescent but active centers around the world.

Acknowledgments. Synthetic Aperture Radar data was provided by the European Space Agency through their North American distributors, Eurimage and SpotImage. The WInSAR consortium acquired and purchased much of the data with funding from NASA, NSF and USGS. Jim Savage, Marianne Guffanti, William Scott, Geoff Wadge and Charles Williams gave helpful comments. Generic Mapping Tools by P. Wessel and W. Smith [*Wessel and Smith*, 1995] were used to construct Figs. 1, 2, and 4.

References

Avallone, A., and P. Briole, Analysis of 5 years of SAR interferometry data from the Gulf of Corinth (Greece), *Eos, Trans. AGU, 81*, F327 , 2000.

Bacon, C.R., Implications of silicic vent patterns for the presence of large crustal magma chambers, *J. Geophys. Res.*, *90*, 11243-11252, 1985.

Blackwell, D., J. Steele, S. Kelley, and M. Korosec, Heat flow in the state of Washington and thermal conditions in the Cascade Range, *J. Geophys. Res.*, *95*, 19495-19516, 1990.

Goldstein, R.M., H.A. Zebker, and C.L. Werner, Satellite radar interferometry: Two-dimensional unwrapping, *Radio Sci.*, *23*, 713-720, 1988.

Guffanti, M., and C.S. Weaver, Distribution of late Cenozoic volcanic vents in the Cascade Range: volcanic arc segmentation and regional tectonic considerations, *J. Geophys. Res.*, *93*, 6513-6529, 1988.

Ingebritsen, S.E., R.H. Mariner, D.E. Cassidy, L.D. Shepherd, T.S. Presser, M.K.W. Pringle, and L.D. White, Heat-flow and water-chemistry data from the Cascade Range and adjacent areas in north-central Oregon, *US Geol. Surv. Open-File Rep.*, *88-702*, 1988

Ingebritsen, S.E., R.H. Mariner, and D.R. Sherrod, Hydrothermal systems of the Cascade Range, north-central Oregon, *US Geol. Surv. Prof. Pap.*, *1044-L*, 86, 1994.

Ingebritsen, S.E., D. Sherrod, and R.H. Mariner, Heat flow and hydrothermal circulation in Cascade Range, north-central Oregon, *Science*, *243*, 1458-1462, 1989.

Iverson, J.T., An investigation of the chloride anomaly in Separation Creek, Lane County, Oregon, B.S. thesis, Oregon State University, Corvallis, OR, 1999.

James, E.R., M. Manga, and T.P. Rose, CO_2 degassing in the Oregon Cascades, *Geology*, *27*, 823-826, 1999.

Lu, Z., C. Wicks, D. Dzurisin, W. Thatcher, J. Freymueller, S. McNutt, and D. Mann, Aseismic inflation of Westdahl volcano, Alaska, revealed by satellite radar interferometry, *Geophys. Res. Lett.*, *27*, 1567-1570, 2000.

Lu, Z., C. Wicks, Jr., D. Dzurisin, J.A. Power, S.C. Moran, and W. Thatcher, Magmatic Inflation at a dormant stratovolcano: 1996-98 activity at Mount Peulik volcano, Alaska, revealed by satellite radar interferometry, *J. Geophys. Res.*, in press, 2002.

Massonnet, D., and T. Rabaute, Radar Interferometry -- Limits and Potential, *IEEE Trans. Geosci. Rem. Sensing*, *31*, 455-464, 1993.

Mogi, K., Relations between the eruptions of various volcanoes and the deformations of the ground surface around them., *Bull. Earthquake Res. Inst. Univ. Tokyo*, *36*, 99-134, 1958.

Scharroo, R., and P.N.A.M. Visser, Precise orbit determination and gravity field improvement for the ERS satellites, *J. Geophys. Res.*, *103*, 8113-8127, 1998.

Scott, W.E., R.M. Iverson, S.P. Schilling, and B.J. Fisher, Volcano hazards in the Three Sisters region, Oregon, *US Geol. Surv. Open-File Report*, *99-437*, (http://geopubs.wr.usgs.gov/open-file/of99-437/), 2001

Sherrod, D.R., and J.G. Smith, Quaternary extrusion rates of the Cascade Range, northwestern United States and southern British Columbia, *J. Geophys. Res.*, *95*, 19465-19474, 1990.

Tarayre, H., and D. Massonnet, Atmospheric propagation heterogeneities revealed by ERS-1 interferometry, *Geophys. Res. Lett.*, *23*, 989-992, 1996.

Taylor, E.M., N.S. MacLeod, D.R. Sherrod, and G.W. Walker, Geologic Map of the Three Sisters Wilderness, Deschutes, Lane, and Linn counties, Oregon, *US Geol. Surv. Misc. Field Studies Map*, MF-1952, 1987.

Wessel, P., and W. Smith, New version of the Generic Mapping Tools released, *EOS Trans. AGU*, *76*, 329, 1995.

White, D.E., L.J.P. Muffler, and A.H. Truesdell, Vapor-dominated hydrothermal systems compared with hot-water systems, *Econ. Geol.*, *66*, 75-97, 1971.

Wicks Jr., C., W. Thatcher, and D. Dzurisin, Migration of fluids beneath Yellowstone caldera inferred from satellite radar interferometry, *Science*, *282*, 458-462, 1998.

Williams, C.A., and G. Wadge, The effects of topography on magma chamber deformation models: Application to Mt. Etna and radar interferometry, *Geophys. Res. Lett.*, *25*, 1549-1552, 1998.

C. Wicks, and W. Thatcher, USGS MS977 345 Middlefield Rd., Menlo Park, CA 94025 (email: cwicks or thatcher@usgs.gov)

D. Dzurisin, USGS, Cascades Volcano Observatory, 1300 SE Cardinal Court, Bldg. 10, Vancouver, WA 98683 (email: dzurisin@usgs.gov)

S. Ingebritsen, USGS MS 472 345 Middlefield Rd., Menlo Park, CA 94025 (email: seingebr@usgs.gov)

Z. Lu, USGS, EROS Data Center, Raytheon, 47914 252nd St., Sioux Falls, SD 57198 (email: lu@usgs.gov)

J. Iverson, Department of Geosciences, Oregon State University, Corvallis, OR 97331 (email: iversonj@geo.orst.edu)

(Received October 10, 2001; accepted January 11, 2002.)

[1]U.S. Geological Survey (USGS), Menlo Park, CA

[2]USGS, Cascades Volcano Observatory, Vancouver, WA

[3]USGS, EROS Data Center, Raytheon, Sioux Falls, SD

[4]Dept. of Geological Sciences, Oregon State Univ., Corvallis, OR

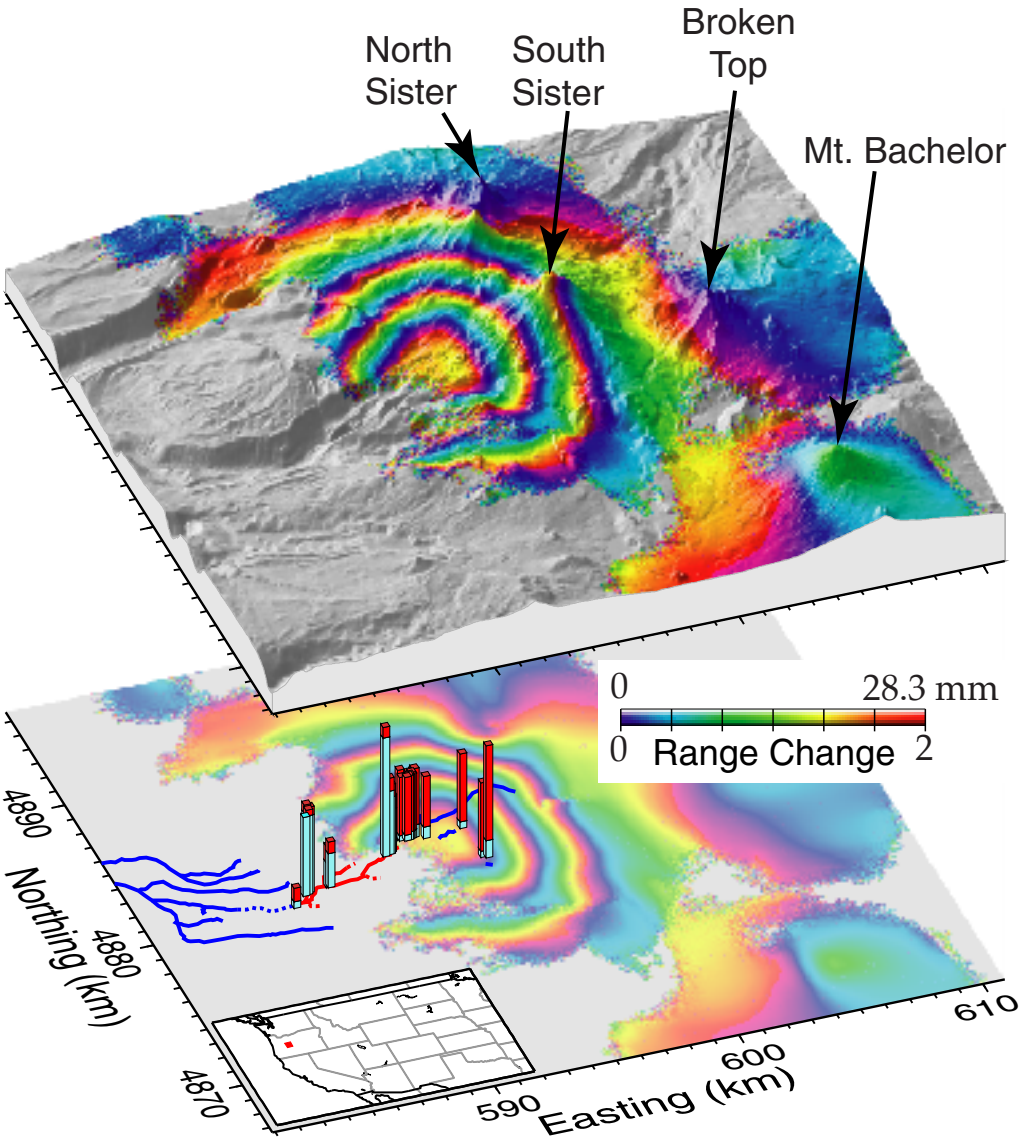

Figure 1. Bottom: A location map (inset, red square shows location of study area) and geochemical data on top of the 1996-2000 interferogram. The columns show chloride and sulfate concentrations at sampled springs. The lengths of the cyan columns depict chloride concentration (0.6 to 18.6 mg/L versus a regional background of 0.2 to 0.7 mg/L). The lengths of the red columns show SO_4/Cl ratios (0.2 to 2.8). Blue lines highlight stream reaches with steady or decreasing Cl concentration in a downstream direction. Red lines highlight reaches within which Cl concentrations increase downstream. The color bar, which applies to all interferograms in this study, shows a range increase from 0 to 28.3 mm that corresponds to a continuous color change from violet to red. **Top:** 1996-2000 interferogram draped over a 30-m DEM.

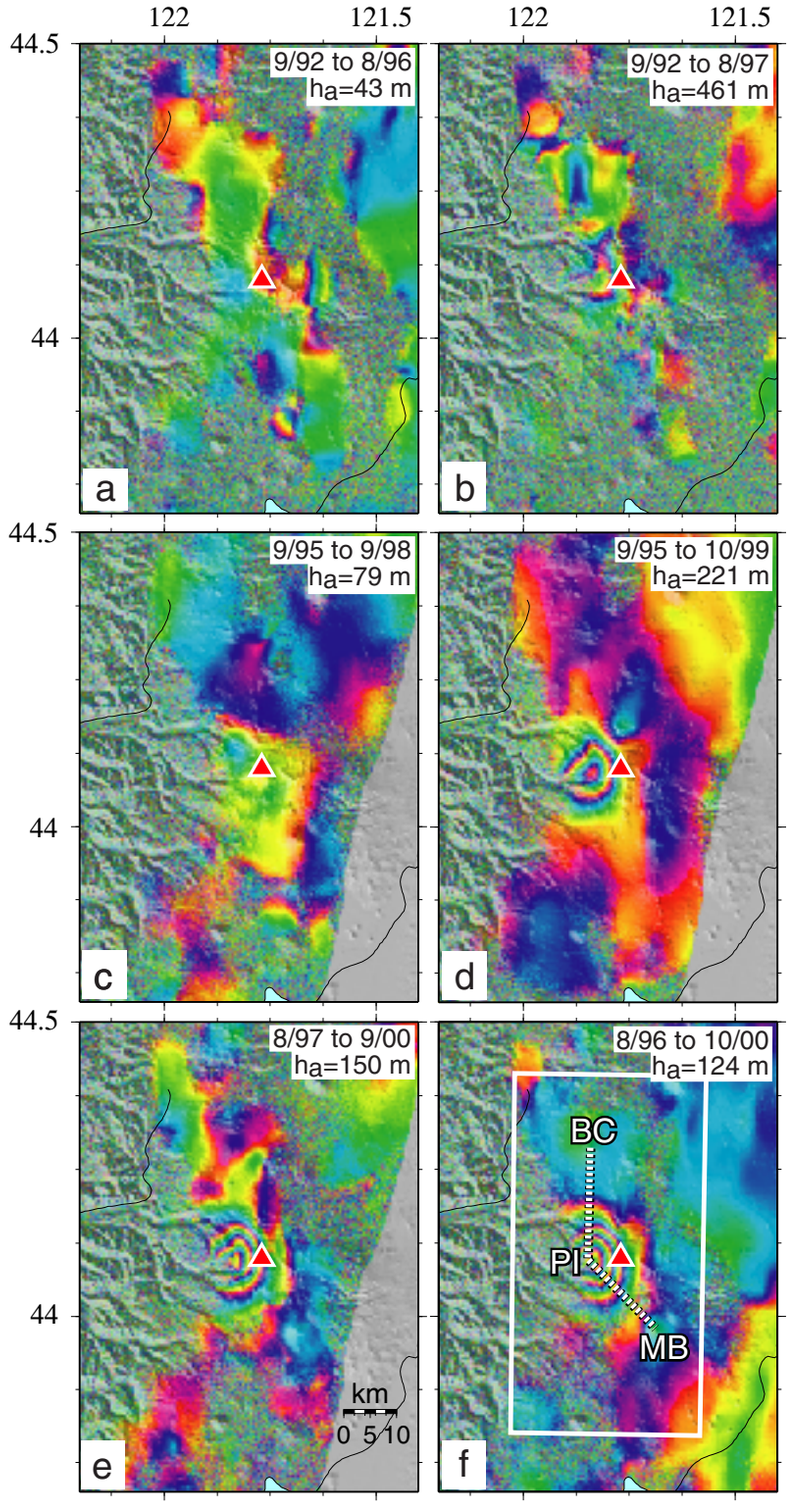

Figure 2. Six 90-m pixel interferograms that show the time history of the uplift. The altitude of ambiguity h_a is the amount of topographic change required to generate one interferometric fringe [*Massonnet and Rabaute,* 1993]. The red triangle marks the location of the summit of South Sister volcano. The scale bar in the bottom right of Fig. 2e applies to all panels. **(a)** September 26, 1992 to August 20, 1996. **(b)** September 26, 1992 to August 5, 1997. **(c)** September 23, 1995 to September 13, 1998. **(d)** September 24, 1995 to October 3, 1999. **(e)** August 24, 1997 to September 17, 2000. **(f)** August 20, 1996 to October 3, 2000. The dashed line running from Belknap Crater (BC) to the approximate maximum point of inflation (PI) to Mount Bachelor (MB) marks the location of deformation profiles detailed in Fig. 3. The white rectangular box delineates the area modeled with 30-m pixel interferograms in Fig. 4.

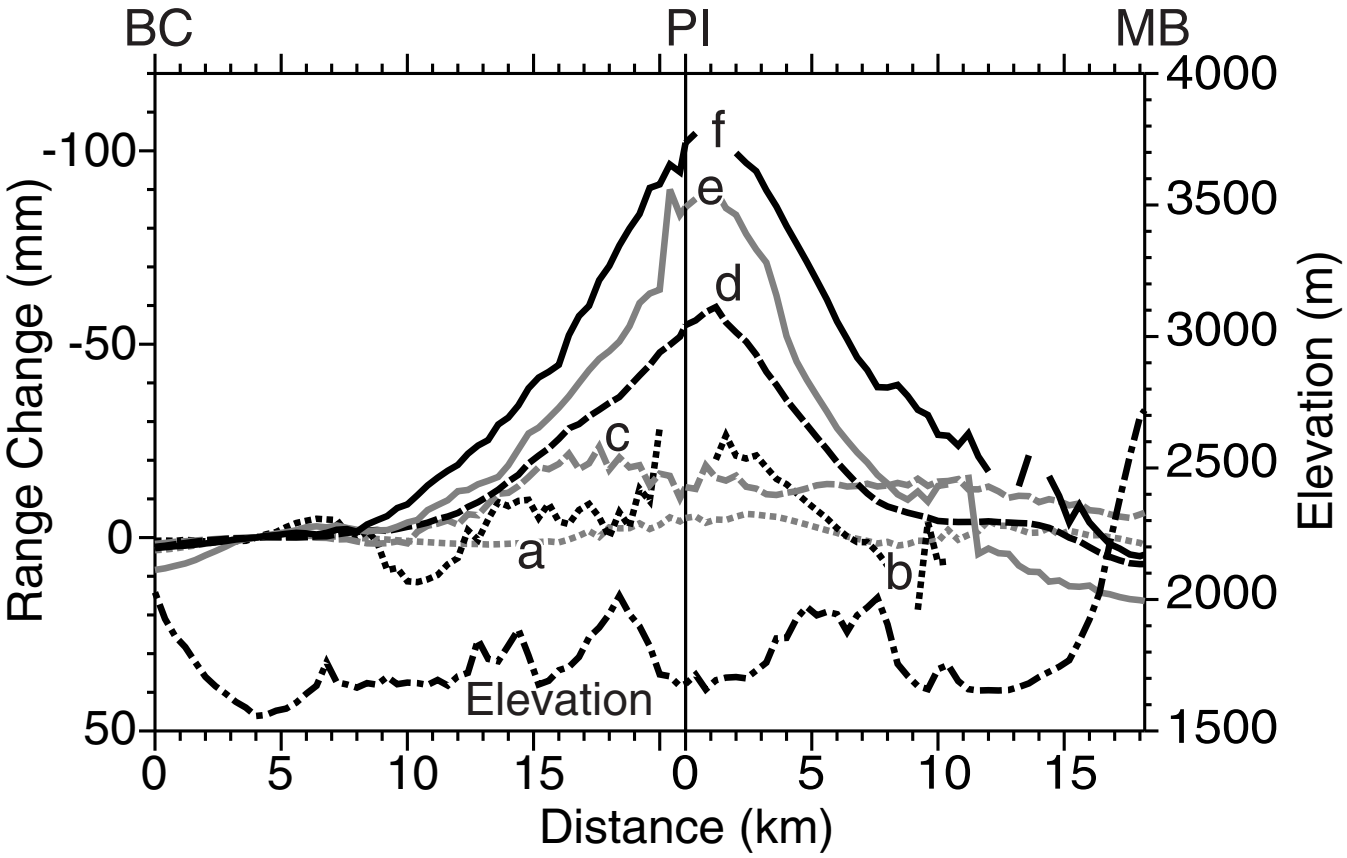

Figure 3. Deformation profiles across unwrapped versions of the interferograms in Fig. 2. Since the interferometric phase is measured modulo 2 , the line-of-sight range change is found by unwrapping the interferograms [*Goldstein et al.,* 1988]. The individual profiles are labeled with the panel descriptor (a-f) from the corresponding interferogram in Fig. 2. The location of the profiles is shown in Fig. 2f. Each profile is referenced (zeroed) to a point on the profile 4 km south of BC (Fig. 2f) on a relatively smooth segment of the profiles outside the area of inflation. The dot-dashed line (bottom) indicates the elevation along the profiles.

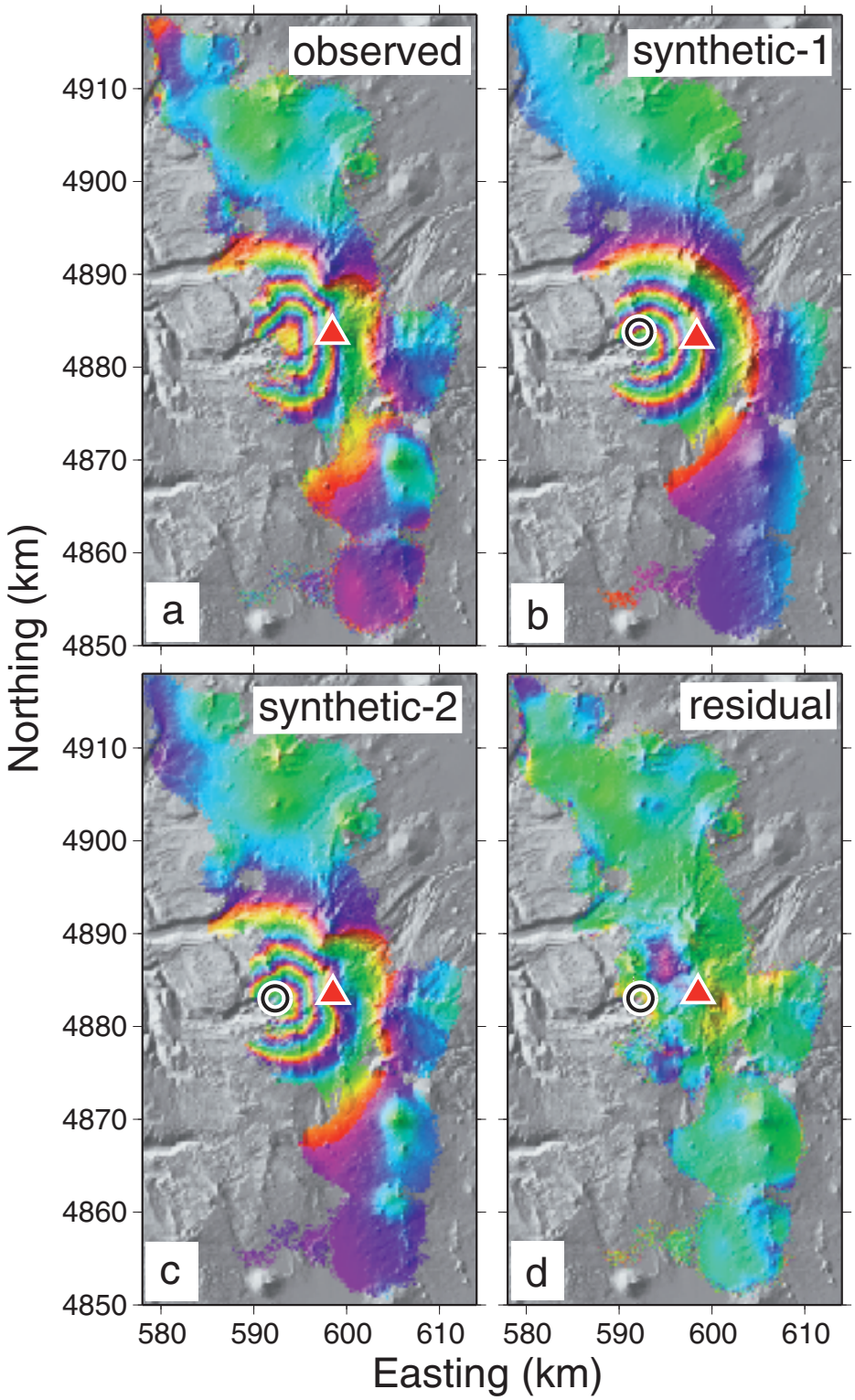

Figure 4. Results from modeling the interferogram in Figs. 1 and 2f. The red triangle shows the location of the summit of South Sister volcano. The circle marks the location of the modeled point source. **(a)** Interferogram for August 1996 to October 2000 pair processed at 30 m pixel size. The colored pixels are those with coherent phase values that were successfully unwrapped. **(b)** Synthetic interferogram generated from the point source model that best fit the data in Fig. 4a where we inverted for seven model parameters and a topography correction (as explained in text). **(c)** Synthetic interferogram with the seven model parameters in Fig. 4b, keeping the topography correction, with the addition of a parameter effecting a tropospheric correction. **(d)** Residual of observed (Fig. 4a) minus synthetic-2 (Fig. 4c).